Frontispiece: New Insight into the Hydrocarbon-Pool Chemistry of the Methanol-to-Olefins Conversion over Zeolite H-ZSM-5 from GC-MS, Solid-State NMR Spectroscopy, and DFT Calculati...

9 AUTHORS, INCLUDING:

Chu Yueying
Wuhan Institute of Physics and Mathematics
24 PUBLICATIONS **243** CITATIONS

Anmin Zheng
Chinese Academy of Sciences
104 PUBLICATIONS **1,584** CITATIONS

Jun Xu
Wuhan Institute of Physics and Mathematics
77 PUBLICATIONS **1,339** CITATIONS

Qiang Wang
Wuhan Institute of Physics and Mathematics
39 PUBLICATIONS **636** CITATIONS

■ Hydrocarbon-Pool Chemistry

New Insight into the Hydrocarbon-Pool Chemistry of the Methanol-to-Olefins Conversion over Zeolite H-ZSM-5 from GC-MS, Solid-State NMR Spectroscopy, and DFT Calculations

Chao Wang,[a] Yueying Chu,[a] Anmin Zheng,[a] Jun Xu,*[a] Qiang Wang,[a] Pan Gao,[a] Guodong Qi,[a] Yanjun Gong,[b] and Feng Deng*[a]

These are not the final page numbers! ↗↗

Abstract: Over zeolite H-ZSM-5, the aromatics-based hydrocarbon-pool mechanism of methanol-to-olefins (MTO) reaction was studied by GC-MS, solid-state NMR spectroscopy, and theoretical calculations. Isotopic-labeling experimental results demonstrated that polymethylbenzenes (MBs) are intimately correlated with the formation of olefin products in the initial stage. More importantly, three types of cyclopentenyl cations (1,3-dimethylcyclopentenyl, 1,2,3-trimethylcyclopentenyl, and 1,3,4-trimethylcyclopentenyl cations) and a pentamethylbenzenium ion were for the first time identified by solid-state NMR spectroscopy and DFT calculations under both co-feeding ([$^{13}C_6$]benzene and methanol) conditions and typical MTO working (feeding [^{13}C]methanol alone) conditions. The comparable reactivity of the MBs (from xylene to tetramethylbenzene) and the carbocations (trimethylcyclopentenyl and pentamethylbenzium ions) in the MTO reaction was revealed by ^{13}C-labeling experiments, evidencing that they work together through a paring mechanism to produce propene. The paring route in a full aromatics-based catalytic cycle was also supported by theoretical DFT calculations.

Introduction

The decreasing of the oil reserves with soaring of the price is exerting great impact on the production of crude oil-based chemicals including industrially important light olefins (e.g., ethene and propene). Because methanol can be produced from other reserves such as coal, natural gas, and biomass, the methanol-to-olefins (MTO) process on acidic zeolite catalysts has attracted increasing attention since the early 1970s because of its potential for providing an alternative for the production of the light olefins.[1] Among all zeolites with different topology, ZSM-5 and SAPO-34 are featured by their distinct selectivity in the MTO process and thus, the central focus of the catalysts for MTO studies, with the former predominantly generating propene[2] and the later producing ethene and propene.[3] Although the MTO process has been successfully commercialized in the context of hydrocarbon formation, the complex reaction network involves methylation, alkylation, oligomerization, and cracking etc., making the definite mechanism elucidation of the olefins formation a challenging topic of considerable debate over the past 40 years.[4] A direct route was initially proposed to account for the first C—C bond formation through methanol or dimethyl ether (DME) C1 species.[4a, 5] However, theoretical calculations indicate a prohibitively high energy of the transition states and the instable intermediates involved in this route,[6] and the less importance of this route

was confirmed by experimental evidence.[7] On the contrary, an indirect route (hydrocarbon-pool mechanism),[8] has been widely accepted for providing a rationale for the light olefins formation.

The hydrocarbon-pool mechanism that was first introduced by Dahl and Kolboe describes a catalytic cycle in which methanol and/or DME react with certain hydrocarbons trapped in a zeolite in a sequence of steps of methylation, followed by the formation of olefins like ethene and propene.[9] The hydrocarbon pool was further developed by Svelle et al. They proposed a "dual-cycle" model for the formation of light olefins on H-ZSM-5,[10] in which ethene was formed through an aromatics-based cycle (involving xylene, trimethylbenzene, and tetramethylbenzene), whereas propene was generated through a C_{3+} alkene methylation/cracking cycle (alkene-based cycle). The prevalence of the "dual–cycle" model in the MTO reaction was also proven on ZSM-22[11] and the zeo-type material SAPO-5.[12] Polymethylbenzenes (MBs) and their protonated counterparts (or other related cyclic species) confined in the voids of zeolites were proposed to serve as the hydrocarbon-pool species and play a co-catalysis role in the methanol-to-hydrocarbon (MTH),[13] methanol-to-gasoline (MTG),[14] and the MTO[15] reaction. The reactivity of various methylbenzenes as hydrocarbon-pool species has been well correlated with the product distribution. For example, in SAPO-34, highly methylated MBs (from tetramethylbenzene to hexamethylbenzene) were correlated to the formation of propene, whereas the formation of ethene was favored by lowly methylated MBs with two or three methyl groups.[15a] On the basis of the MBs and their protonated counterparts (e.g., benzenium ions), two different aromatics-based routes were proposed for the operation of the hydrocarbon-pool mechanism.[16] One is the side-chain methylation route, which describes the formation of light olefins by elimination of the alkyl chain that is generated by repeated methylation of aromatics,[8d,e, 17] and the other, paring route, proposes a ring contraction and expansion of a benzenium ion, resulting in the formation of an alkyl chain and its subsequent splitting to produce light olefins.[13g, 18]

For the identification of active hydrocarbon-pool species, carbon isotopic labeling experiments are commonly used, and carbon label scrambling observed by gas chromatography–mass spectroscopy (GC-MS) in the olefins and the polymethyl-

[a] C. Wang,+ Dr. Y. Chu,+ Dr. A. Zheng, Dr. J. Xu, Dr. Q. Wang, P. Gao, G. Qi, Prof. Dr. F. Deng
Wuhan Center for Magnetic Resonance, State Key Laboratory Magnetic Resonance and Atomic Molecular Physics
Wuhan Institute of Physics and Mathematics
Chinese Academy of Sciences, Wuhan 430071 (P.R. China)
Fax: (+86)27-87199291
E-mail: xujun@wipm.ac.cn
       dengf@wipm.ac.cn

[b] Prof. Y. Gong
State Key Laboratory of Heavy Oil Processing
CNPC Key Laboratory of Catalysis
China University of Petroleum-Beijing
Beijing 102249 (P.R. China)

[+] Both authors contributed equally to this work.

🖥 Supporting information for this article (containing experimental and theoretical calculation details) is available on the WWW under http://dx.doi.org/10.1002/chem.201403972.

↖↖ These are not the final page numbers!

benzenes may provide clues on the hydrocarbon-pool mechanism,[4c] which however is not conclusive for the determination of the specific reaction pathway. The coexistence of different scrambling routes may make the isotopic label distribution complicated and thus the corresponding reaction route uncertain. Solid-state NMR spectroscopy is a powerful tool for the identification of active species,[19] especially the long-lived carbocations in catalytic reactions.[4b] Observation of C_5- and C_6-cyclic carbocations in the MTO reaction might provide key mechanistic information about the two pathways (paring and side-chain methylation routes). According to NMR spectroscopic results, these two routes were proposed for the formation of propene on SSZ-13 zeolite (with a CHA topology).[20] Therefore, it is essential to observe and identify the key hydrocarbon-pool species or intermediates, on basis of which the implicated mechanism reconciles the distribution of expected products and the isotopic labeling in the full catalytic cycle in the MTO conversion.

With respective to H-ZSM-5, the hydrocarbon-pool mechanism has been widely explored by co-reaction of aromatics and methanol or DME through isotopic labeling.[4e, 8d, 13a, 21] Most recently, the effect of co-feeding of aromatics on the distribution of ethene and propene was systematically investigated by Lercher and co-workers.[22] In addition, Bhan et al.[21] demonstrated that tetramethylbenzene was the preferable precursor to ethene and propene in H-ZSM-5 zeolite. Parallel to the experimental works, McCann et al. carried out the first theoretical study to rationalize the formation of isobutene on H-ZSM-5 by connecting MBs and previously observed cyclopentenyl and benzenium ions.[23] Additionally, Lesthaeghe et al.[24] theoretically studied the formation of ethene and proposed the aromatics-based side-chain route though a high energy barrier was required to eliminate ethene from aromatics.

Up to now, although MBs are believed as particularly important hydrocarbon-pool species in the H-ZSM-5 zeolite, the detailed aromatics-based mechanism still remains unclear, due to the lack of direct observation of the key intermediates in the MTO process. In this work, the MTO reaction occurring in zeolite H-ZSM-5 was comprehensively studied by GC-MS, solid-state NMR spectroscopy, and theoretical calculations. To probe the active intermediates and the aromatics-based pathway, co-feeding methanol and benzene as well as typical methanol conversions were performed under both pulse-quench and continuous-flow modes. We report for the first time the simultaneous observation and identification of the cyclopentenyl cations **1**–**3** (see Scheme 1) and the pentamethylbenzenium ion **4** in the MTO process over zeolite H-ZSM-5. A paring route correlating the MBs with the olefin products through these carbocations is accordingly proposed for the formation of propene. Moreover, our theoretical calculations also support the paring route in a full catalytic cycle, which has a much lower reaction barrier with respect to the side-chain methylation route. Therefore, the results presented herein shed new insights into the hydrocarbon-pool chemistry of the MTO reaction over zeolite H-ZSM-5.

Results and Discussion

Reactivity of MBs in the initial stage

It is a consensus that the light olefins are formed in the very early stage, and their rapid secondary reactions lead to a complex reaction network prevailing under the steady-state condition.[4a] In order to reveal the most possible pathway for the origin of the primary olefins, the products formed in the initial stage were analyzed by GC-MS. The reaction was quickly quenched by liquid nitrogen within a short period (< 1 s), which allows the investigation of the reaction during the induction period. Moreover, a high feed rate (500 mL min^{-1}) was utilized to suppress the secondary reactions. After reacting methanol on H-ZSM-5 for 4 s at 350 °C, the conversion yield is as low as 5% (Figure S1 in the Supporting Information) and the formation of light olefins is negligible, but a considerable amount of aromatics is already present, with MBs ranging from toluene to pentamethylbenzene being predominant in the extract of the trapped species. To gain insight into the role of the MBs particularly in the initial stage of the MTO reaction, their reactivity was studied by co-reaction of benzene and methanol in a short period (up to 16 s). A mole ratio of 2–4 was used in our co-feeding experiments. Under the steady-state condition, a wide range of methanol/DME-to-benzene co-feeding ratio ($\approx$0.7–8:1) was employed in the previous work[4e, 8d, 12, 13, 21] to link ethene and propene to aromatics or its derivatives. According to the work of Lercher and co-workers,[22] even at a very low concentration of co-fed aromatics (2–4 mol.% benzene, toluene, or *p*-xylene), the aromatics-based cycle was notably promoted, whereas the alkene-based cycle was significantly suppressed. Therefore, the co-feeding reaction allows us to detect the active species mainly derived from the MBs and to analyze the reaction pathway associated with the aromatics-based catalytic cycle. As expected, the MBs due to facile methylation of benzene dominated the products (Figures S2 and S3 in the Supporting Information). Isotropic labeling analysis was performed on both the trapped MB species and the formed olefins by using [$^{13}C_6$]benzene and methanol. Figure 1 shows a typical result for the trapped tetramethylbenzene and those for other MBs can be found in Figure S4 in the Supporting Information. Generally, the mass spectra of MBs derived from the co-reaction of [$^{13}C_6$]benzene with unlabeled methanol show similarity in the mass distribution to those of MBs generated from the co-reaction of unlabeled benzene with unlabeled methanol, but the corresponding mass unit of the MBs shifts to higher *m/z* values by six (see Figure 1 a). The six ^{13}C atoms in the phenyl ring of the MBs accounts for such a change in the mass unit. This implies that the methyl groups of the MBs
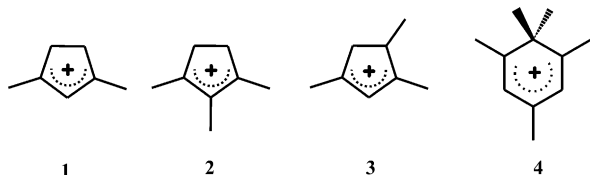
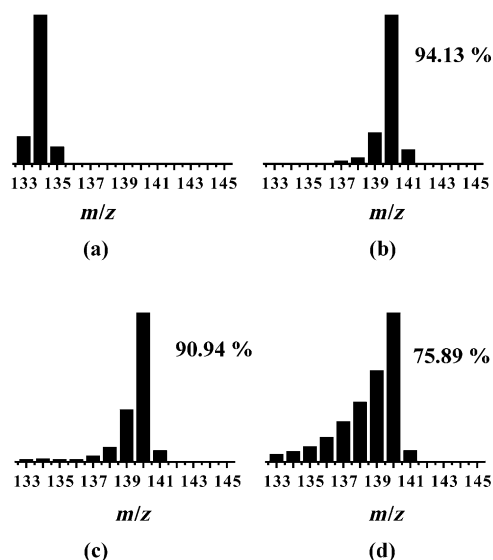**Scheme 1.** Carbocations observed by solid-state NMR spectroscopy.

These are not the final page numbers! ↗↗

Figure 1. Mass spectra of the trapped tetramethylbenzene obtained from the co-reaction of $[^{13}C_6]$benzene (or benzene) with methanol over H-ZSM-5 at 300 and 400 °C for various times. The ^{13}C content (%) is given. a) Methanol and benzene, 300 °C, 4 s; b) methanol and $[^{13}C_6]$benzene, 300 °C, 4 s; c) methanol and $[^{13}C_6]$benzene, 300 °C, 16 s; and d) methanol and $[^{13}C_6]$benzene, 400 °C, 16 s.

Figure 2. Isotopic distribution in ethene (top) and propene (bottom) in the effluent products obtained from co-reaction of $[^{13}C_6]$benzene with methanol over H-ZSM-5 at 300 °C for various times. Green = 4, red = 8, and blue = 16 s.

are mainly formed by the methylation of ^{13}C-labeled benzene with unlabeled methanol. More interestingly, some m/z peaks at the downward part of the molecular ion peak are observable for the ^{13}C-containing trapped MBs. For example, new peaks at $m/z = 137$ and 138 appear for the trapped tetramethylbenzene (Figure 1 b). This can be attributed to the incorporation (isotopic scrambling) of two or three ^{12}C atoms of unlabeled methanol into the ^{13}C-labeled phenyl ring, leading to the broad mass distribution. A similar phenomenon can be found for other ^{13}C-containing MBs (see Figure S4 in the Supporting Information). It should be noted that increasing the reaction time from 4 to 16 s at 300 °C results in a much broader mass distribution of tetramethylbenzene, implying that more ^{12}C atoms of unlabeled methanol are involved in the isotopic scrambling. Additionally, a higher reaction temperature (400 °C) leads to a remarkable decrease of the ^{13}C content in the phenyl ring, from approximately 91 % at 300 °C to 76 % at 400 °C (Figures 1 c and d). A similar phenomenon was found for the other MBs (Figure S4 in the Supporting Information).

To trace the ^{13}C atom, we also analyzed the isotopic composition of the light olefins by MS. As shown in Figure 2, the ^{13}C-incorporated olefins dominate the isotopomers of both ethene and propene that are the main olefin products detectable at 300 °C. Importantly, nearly 90 % of the effluent ethene and propene contains one or more ^{13}C atoms after 4 s. The origin of the ^{13}C atom in the light olefins can be definitely attributed to the ^{13}C-labeled phenyl ring of the trapped MBs, implying that the pre-formed MBs account for the initial formation of the light olefins in the induction period. Further analysis shows that propene that contains one ^{13}C atom derived from the phenyl ring of MBs and two ^{12}C atoms from methanol is predominant in the distribution of the isotopomers, which
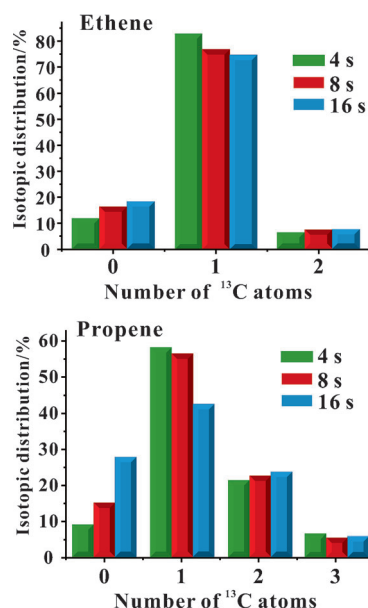
amounts to 58 % at a reaction time of 4 s and 42 % at a reaction time of 16 s. For ethene that contains one ^{13}C atom derived from MBs and one ^{12}C atom from methanol, the corresponding values are 83 and 75 %, respectively. Thus, the paring mechanism is presumably prevailing at least within a reaction time of 16 s for both propene and ethene. This route is consistent with the prediction that MBs produce propene with one C atom originating from the phenyl ring and the other C atoms from the substituted alkyl groups that comes from methanol. The results here demonstrate that the paring mechanism can operate even in the initial period in the MTO reaction. The modest amount of propene containing two or three ^{13}C atoms might suggest the simultaneous operation of competitive reactions including an oligomerization/cracking reaction of olefins.[8b,c] In line with the previous work,[22] the alkene-based cycle contributing to the parallel formation of olefins cannot be completely suppressed in the reaction by co-feeding aromatics. The oligomerization of ^{13}C-labeled propene or ethene and its subsequent cracking would lead to enrichment in the ^{13}C atoms. However, this process would not be pronounced, reflected by the lower content of such propene isotopomers with enriched ^{13}C atoms (28 % at 4 s and 30 % at 16 s of the total propene isotopomers). Moreover, we found that the total ^{13}C content in ethene and propene at reaction time of 4 s is similar (47 versus 40 %), indicating that the formation of propene is not due to methylation of ethene with ^{13}C-unlabeled methanol. Otherwise, more ^{12}C-atom-containing propene isotopomers and a much lower total ^{13}C content should be expected. In fact, the methylation of ethene was found to have a remarkably low rate and be not pronounced in the MTO process in comparison with the methylation of C_{3+} olefins, for example, propene and butene.[25] Thus, in the aromatics-based catalytic cycle, the paring mechanism should be the main pathway for the forma-

tion of both propene and ethene, particularly in the initial stage.

Observation and identification of carbocations

The paring mechanism for the formation of propene from MBs is featured by a 6↔5 ring contraction/expansion process through C_5- or C_6- cyclic carbocation intermediates.[13g, 18, 23] The observation and identification of these active intermediates would provide direct evidence for the operation of the paring pathway. Solid-state NMR technique was used to detect the trapped species, in which long-lived carbocations could be readily differentiated from the MBs by their characteristic low-field chemical shifts.[13d,e, 14, 26] The MTO reactions under different conditions were rapidly quenched and examined with solid-state NMR spectroscopy. After the co-reaction of [$^{13}C_6$]benzene with methanol for 16 s at 275 °C (Figure 3a), a strong and unsymmetrical signal at $\delta = 134$ ppm with a shoulder peak at $\delta \approx 140$ ppm was observed, due to the unsaturated hydrocarbon species. Three weak but well-resolved signals appeared at $\delta = 205$, 189, and 58 ppm. Taking the three signals and the $\delta = 140$ ppm signal into account together, the formation of the pentamethylbenzenium ion **4** can be unambiguously confirmed, in line with the previous NMR data.[14b] Increasing the reaction temperature to 300 °C accelerated the formation of cation **4** (Figure 3b). When the temperature further went up (Figures 3c–h), a series of weak lower-field signals in the chemical shift range of $\delta = 243$–256 ppm appeared. According to the chemical shifts, some cyclic carbocations were expected to be formed.[4b] In order to identify the role of the cation **4** in the formation of olefins, reactions were performed at 400 °C for different reaction times. At 400 °C, in the isotopomers, one ^{13}C atom-containing propene molecule was predominant at 400 °C ($\approx 45\%$) before 8 s and still over 40% at 16 s (Figure S5 in the Supporting Information). Thus, the underlying paring route for the formation of propene from MBs was still prominent at this temperature. As can be seen from the ^{13}C cross polarization magic angle spinning (CP/MAS) NMR spectra (Figures 3d–f), the signals of the cyclic carbocations at $\delta = 243$–256 ppm were gradually growing with the reaction time being increased from 4 to 16 s. For an accurate analysis, these carbocations were produced with a relatively high concentration by changing the ratio of methanol to [$^{13}C_6$]benzene from 2:1 to 4:1, which may facilitate the methylation of benzene to generate more cyclic carbocations. After reaction for 8 s, at least four signals could be resolved at $\delta = 243$, 247, 250, and 256 ppm in the ^{13}C NMR spectrum (Figure 3g). In addition, two shoulder signals at $\delta = 143$ and 147 ppm were notably pronounced and a weak signal at $\delta = 155$ ppm could be discerned. The appearance of these signals evidences the formation of cyclopentenyl cations. Specifically, the signals at $\delta = 250$ and 147 ppm can be ascribed to the allyl cation moiety of the 1,3-dimethylcyclopentenyl cation **1**,[14a] the signals at $\delta = 243$ and 155 ppm to the similar allyl moiety of the 1,2,3-trimethyl-cyclopentenyl cation **2**,[27] whereas the signals at $\delta = 247$, 256, and 143 ppm are tentatively assigned to the allyl cation moiety of the 1,3,4-trimethyl cyclopentenyl cation **3**. The meth-
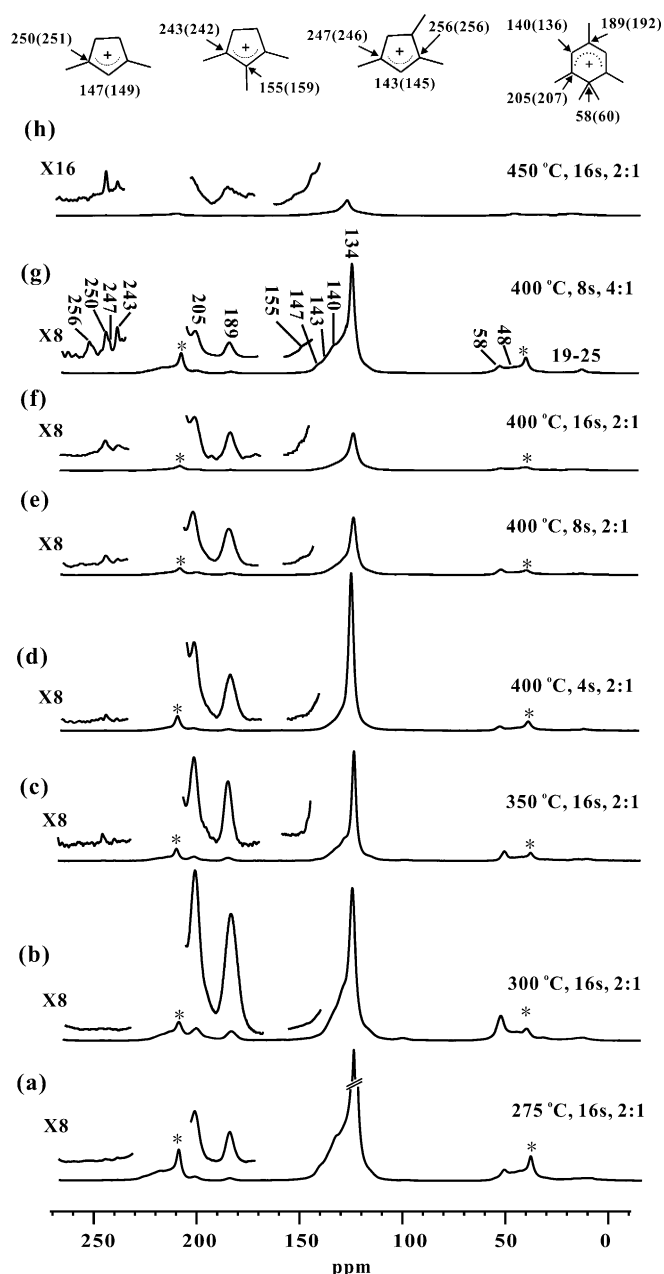

Figure 3. ^{13}C CP/MAS NMR spectra of the products obtained from co-reaction of [$^{13}C_6$]benzene with methanol over H-ZSM-5 at different reaction temperatures. The mole ratio of methanol to benzene is 2:1 or 4:1. The calculated ^{13}C chemical shifts are given in parenthesis. Asterisks denote spinning sidebands.

ylene moieties that possess a similar chemical environment in these cyclopentenyl cations give rise to the signal at $\delta = 48$ ppm. These assignments are also supported by our DFT calculations. The calculated ^{13}C chemical shifts of these cyclopentenyl cations are in good agreement with the experimental values (see Table 1). Increasing the temperature to 450 °C resulted in a further decrease of both the cyclopentenyl cations and the pentamethylbenzenium ion (Figure 3h), indicative of their high reactivity at a higher temperature.

It is noteworthy that the concentration of the pentamethyl-benzenium ion **4** characterized by the signals at $\delta = 189$ and

These are not the final page numbers! ↗↗

Table 1. Calculated and experimentally observed ^{13}C chemical shifts of the carbocations. The number of the appropriate carbon atoms are given in parenthesis.

Carbocation	Calculated δ [ppm]	Experimental δ [ppm]
1	251 (1, 3)	250 (1, 3)
	149 (2)	147 (2)
	52 (4, 5)	48 (4, 5)
2	242 (1, 3)	243 (1, 3)
	159 (2)	155 (2)
	50 (4, 5)	48 (4, 5)
3	246 (1)	247 (1)
	145 (2)	143 (2)
	256 (3)	256 (3)
	62 (4)	58 (4)
	55 (5)	58 (5)
4	207 (1,3)	205 (1,3)
	60 (2)	58 (2)
	136 (4,6)	140 (4,6)
	192 (5)	189 (5)

Figure 4. Gas chromatography analyses of the trapped products obtained from co-reaction of benzene with methanol over H-ZSM-5 at 400 °C for various times (a–c). The molar ratio of methanol to benzene is 2:1. The transformations from the carbocations to the corresponding conjugated bases are also illustrated.

205 ppm was gradually decreased, whereas a slight growth of the cyclopentenyl cations was evident with the increase of the reaction time at 400 °C (Figures 3 d–f). This implies that there is some extent of transformation between the C_5- and C_6-cyclic carbocations, in which the benzenium ion such as the cation **4** may serve as the precursor of the cyclopentenyl cations. Importantly, the presence of cation **3** in the H-ZSM-5 zeolite is for the first time experimentally identified and confirmed δ DFT calculation, which would provide new information on the hydrocarbon-pool chemistry.

The presence of the aforementioned C_5- and C_6-cyclic carbocations is also supported by GC-MS experiments. These carbocations would be deprotonated to form their corresponding conjugated bases during the extracting process (see the Experimental Section). As shown in Figure 4, the GC-MS spectra of the extracts indeed confirm the presence of 1) 1,3-dimethyl-1,3-cyclopentadiene (1,3-diMCP), 2) 1,2,3-trimethyl-1,3-cyclpentadiene (1,2,3-triMCP), 3) 1,2,4-trimethyl-1,3-cyclpentadiene (1,2,4-triMCP), and 4) 1,5,6,6-tetramethyl-4-methylene-1,4-cyclohexadiene (1,5,6,6-tetraMMC), corresponding to the conjugated bases of cations **1**, **2**, **3** and **4**, respectively. Moreover, the assignment of the former three species was further supported by recording the GC spectra of deliberately synthesized compounds (see Figure S6 in the Supporting Information for more details). Therefore, we can conclude that the cyclopentenyl cat-
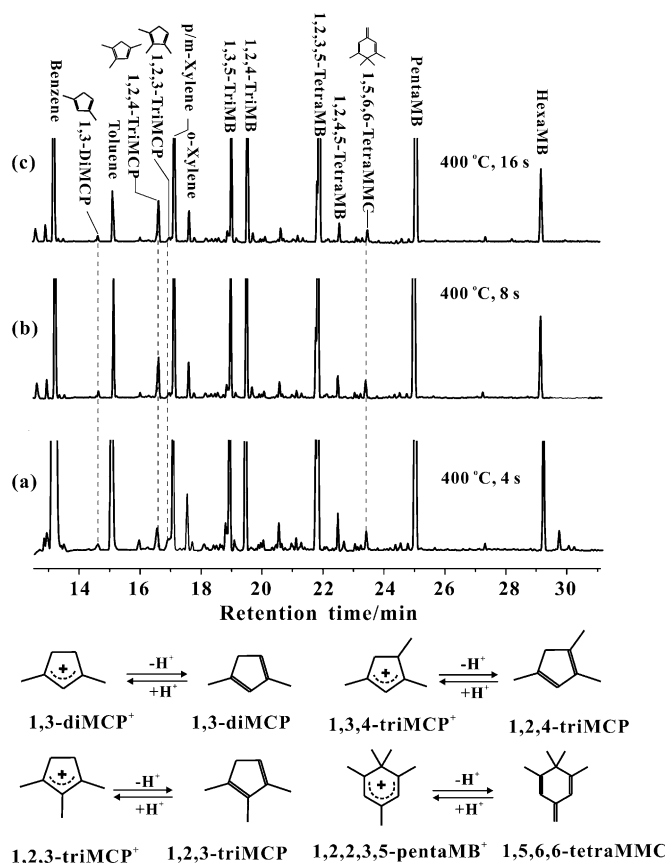
ions and the pentamethylbenzenium ion are simultaneously generated in the induction period of the MTO reaction.

Identification of these carbocations was extended to a typical MTO reaction at various temperatures under continuous-flow conditions in which [^{13}C]methanol was fed alone. At 275 °C, a low methanol conversion was evidenced by the presence of a plenty of dimethyl ether ($\delta = 60$ ppm) and methanol ($\delta = 50$ ppm) (Figure 5 a). Despite the low methanol conversion, the formation of cation **4** was confirmed by the appearance of the $\delta = 189$ and 205 ppm signals. It should be noted that a relatively larger amount of cation **4** was produced in the co-feeding reaction at the same temperature but for much shorter reaction time (16 s). The trapped products were analyzed by GC-MS (Figure S7 in the Supporting Information), showing that a small amount of aromatics was formed at this temperature. Thus, the presence of aromatics promotes the formation of the carbocation intermediates. At elevated temperatures of 300 and 325 °C, the methanol conversion was increased and apart from cation **4**, cations **1–3** were also observable (Figures 5 b and c). Thus, these carbocations are involved in the MTO reaction over zeolite H-ZSM-5 under working conditions. These species were becoming instable reflected by the decrease of their concentration at higher temperatures (Figures 5 d–
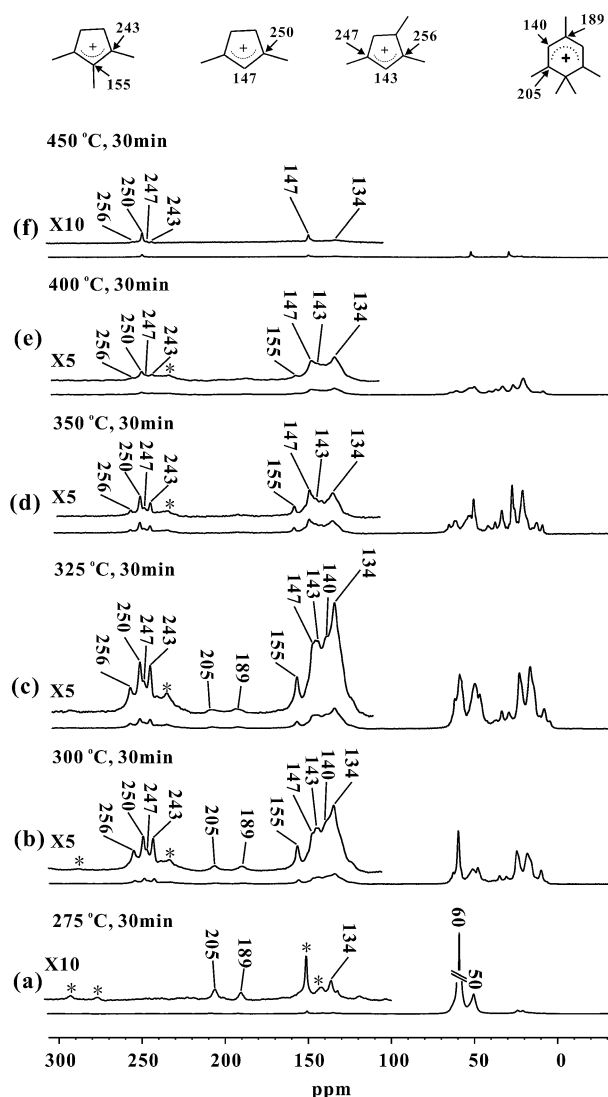
↖↖ These are not the final page numbers!

Figure 5. ^{13}C CP/MAS NMR spectra of the products obtained from the reaction of [^{13}C]methanol over H-ZSM-5 for 30 min at different temperatures. Asterisks denote spinning sidebands.

Figure 6. ^{13}C CP/MAS NMR spectra of the products obtained from the reaction of [^{13}C]methanol over H-ZSM-5 at 300 °C for different reaction times. Asterisks denote spinning sidebands.

f). Taking the co-reaction results into account, the formation and transformation of these carbocations definitely evidence the operation of a paring pathway in the MTO reaction.

The MTO reaction under continuous flow conditions was further studied at 300 °C for various time on stream. After reaction for 5 min, all the above-determined C$_5$- and C$_6$- cyclic carbocations were clearly observed on the H-ZSM-5 zeolites, and they were accumulated along with the reaction process (Figure 6). In order to gain insight into the role of the carbocations formed under working conditions, the methanol conversion was correlated to the evolution of carbocations. The concentration of carbocations was estimated by measuring the integrated peak areas of the corresponding NMR signals. As shown in Figure 7, the concentration of carbocations grew up along with the reaction process, showing a similar variation trend to that of the methanol conversion. This indicates that both the C$_5$- and C$_6$-cyclic carbocations play an intermediate role in the MTO reaction. These carbocations may be associat-
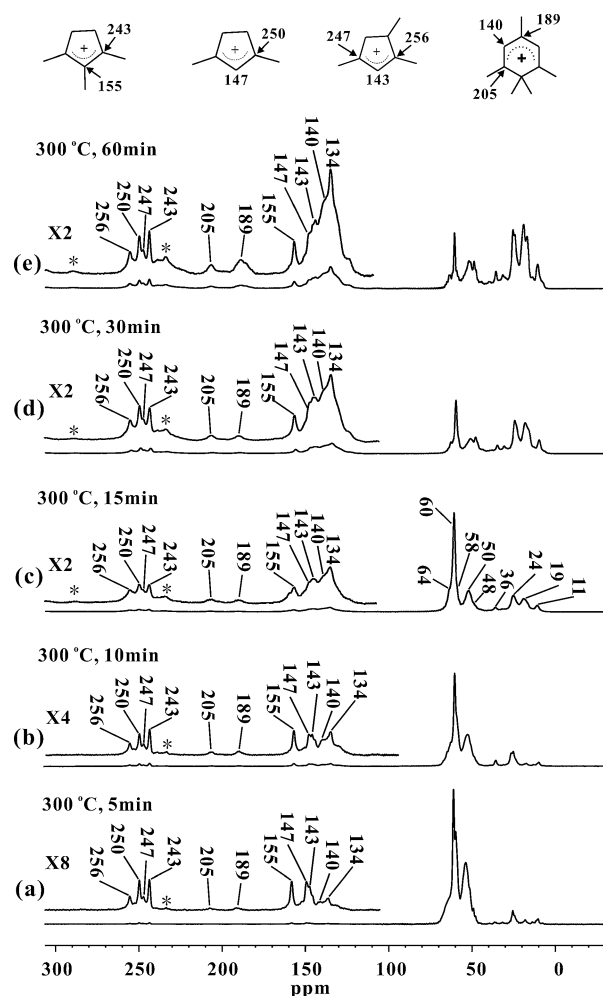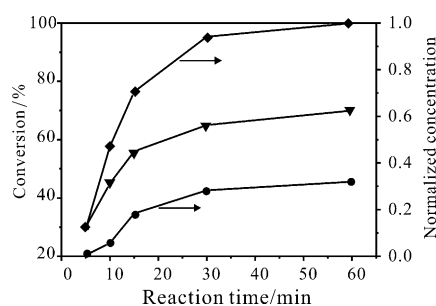
Figure 7. Time evolution of the concentration of the pentamethylbenzenium ion (●) and the cyclopentenyl cations (♦), and the methanol conversion (▼) over H-ZSM-5 at 300 °C. The concentration of the carbocations is normalized to that of the cyclopentenyl cations at 60 min.

ed with the aromatics-based catalytic route to form olefins through the paring mechanism.

Under the MTO working conditions, the evolution of these carbocations was further evaluated by ^{13}C-labeling experiments. The ^{13}C incorporation in these species was monitored

after switching [^{13}C]methanol to unlabeled methanol at 30 min on stream and 300 °C. After the switching the reaction was allowed to proceed for one, two, and four minutes, the ^{13}C content in the extracts of the corresponding conjugated bases (1,2,4-triMCP and 1,5,6,6-tetraMMC) of the carbocations, especially the cations **3** and **4**, show a similar variation trend to that of xylene, trimethylbenzene (triMB), and tetramethylbenzene (tetraMB) trapped in the channels of the H-ZSM-5 zeolite (Figure 8), that is, the concentration variations of cations **3** and
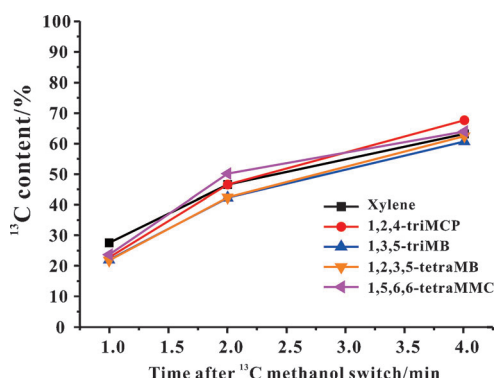

Figure 8. Time evolution of the ^{13}C content in the trapped species obtained from the reaction of methanol for 30 min, followed by switching to [^{13}C]methanol over zeolite H-ZSM-5 at 300 °C. ■ = Xylene, ● = 1,2,4-trimethyl-1,3-cyclpentadiene, ▲ = 1,3,5-trimethybenzene, ▼ = 1,2,3,5-tetramethylbenzene, ◀ = 1,5,6,6-tetramethyl-4-methylene-1,4-cyclohexdiene.

4 are well correlated with those of xylene, trimethylbenzene, and tetramethylbenzene in the MTO process. This experimental result unambiguously demonstrates the similar reactivity of the MBs and the carbocations, and rationalizes the transformation cycle of these species in the proposed reaction pathway (see below).

Aromatics-based reaction pathway

On the basis of the above-described experimental results, we can rationalize the formation of propene through the paring mechanism, in which the ring contraction of the pentamethyl-benzenium ions (i.e., cation **4**) leads to the formation of the 1,3,4-trimethylcyclopentenyl cation **3** by producing propene, followed by the regeneration of MBs through the expansion of cation **3**. The detailed full catalytic cycle for the propene formation was depicted and the calculated energy barriers (in kcal mol^{-1}) were also included in Scheme 2. Starting from the MBs, the pentamethylbenzenium

ion (P3, characterized by cation **4**) is readily formed by methylation of 1,2,3,5-tetraMB (P2), one of the aromatics products formed due to repeated methylation of xylene (P1). Proceeding through a transient state of the 1,3,5,6,6-pentamethylbicyclo-[3.1.0]hexenyl cation (P4), a propyl group is formed due to the ring contraction of the pentamethylbenzenium ions, and subsequently split off as propene with simultaneous formation of the 1,2,4-trimethylcylcopentadienylium cation (P5) that is characterized by cation **3** on the working catalyst. In the following steps, ring expansion of the cyclopentadienylium cation gives rise to the benzenium ion (P7) through the 3-methylbicyclo-[3.1.0]hexenyl cation intermediate (P6). The catalytic cycle ends up with the formation of *m*-xylene (P1) by subsequent deprotonation. It is noteworthy that the step for producing propene (from P4 to P5) has the highest energy barrier (39.55 kcal mol^{-1}), indicating that this is the rate-determining step in the whole catalytic cycle.

The repeated methylation of xylene proceeds readily with the formation of the higher MBs, in which the calculated energy barrier for the formation of tetramethylbenzene from xylene (35.61 kcal mol^{-1}, see Figure S8 in the Supporting Information) is comparable to that for the propene formation step (39.55 kcal mol^{-1}). This strongly suggests the feasibility of the aromatics-based paring route undertaking in the catalytic cycle. It is clear from this route that one propene molecule obtains two carbon atoms from the methyl group, whereas one carbon atom comes from the phenyl ring. This is consistent with the isotopic-labeling experimental result that the singly ^{13}C-atom-containing propene molecule dominates the isotopomers. On the other hand, according to the paring route, the ring expansion of the cyclopentenyl cation leads to the incorporation of the methyl carbon atom from unlabeled methanol into the [^{13}C$_6$]benzene, which accounts for the experimentally observed reduction of the ^{13}C content in the derived MBs. Increasing the reaction time and temperature substantially promotes the cycling of the paring route, which results in the multiple scrambling of the MBs observed in the isotopic-labeling experiments. As an isomer of cation **3**, cation **2** might func-
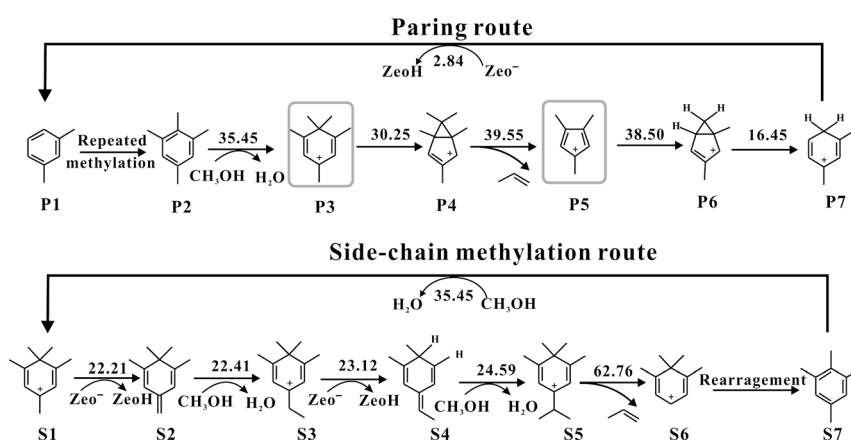
Scheme 2. Full catalytic cycle for the formation of propene through the paring and the side-chain methylation pathway over H-ZSM-5. The calculated energy barriers in kcal mol^{-1} are also given for each step. ZeoH and Zeo$^-$ represent H-form ZSM-5 and deprotonated H-ZSM-5 zeolites, respectively.

tion similarly as the former in the paring route. As one of the key intermediates, the presence of cation **1** supports another paring route proposed by theoretical calculations from McCann and co-workers,[23] in which the cation **1** and the pentamethylbenzenium ion were correlated with polymethylbenzenes in one catalytic cycle to produce isobutene as one of the primary olefins. Under our reaction conditions, a small amount of isobutene was indeed detected. Thus, the simultaneous observation of the cyclopentenyl and pentamethylbenzenium ions points to the paring route for the formation of olefins.

Although our experimental observations agree with the results as expected from the paring route, the side-chain methylation route, which was frequently considered in the MTO reaction[24, 28] was also theoretically studied (see Scheme 2). Among the successive steps for the formation of species from S1 to S7, the highest energy barrier (62.76 kcal mol^{-1}) was found for the slitting of propene (rate-determining step) from the propyl-substituted methylbenzene (S5) that was presumably formed by repeated methylation of aromatics on the phenyl ring and the methyl group (from S1 to S5). This energy barrier is also much higher than the highest one (39.55 kcal mol^{-1}) in the paring route, which corresponds to the step for producing propene. The transition states (TSs) in the rate-determining step of the two routes were further studied by analyzing the noncovalent interactions between the TS species and the zeolite framework, which is realized by visualizing the isosurfaces of the reduced density gradient in real space.[29] As shown in Figure 9, the isosurface of the TS species in the side-chain methylation route exhibits a larger red region, indicating that it suffers a much stronger repulsive interaction from the zeolite framework compared with the TS species in the paring route. The steric constraints imposed by the zeolite framework result in the pronounced repulsive interaction and thus a less stability of the TS species, which accounts for the higher energy required for the side-chain methylation route. Therefore, from the energy point of view, the paring route is much more favorable than the side-chain methylation route. In fact, there is no detectable propyl-substituted tetramethylbenzene (S5) in
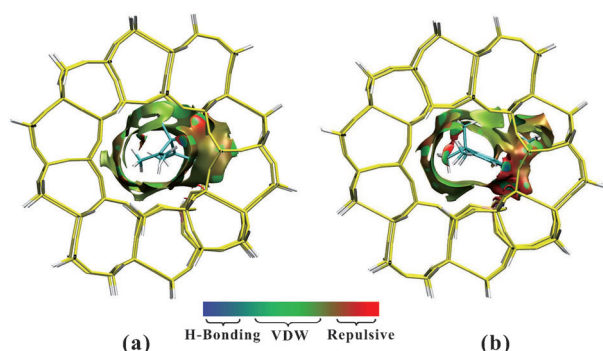

Figure 9. Isosurface plots of the reduced density gradient ($s = 0.500$ au) for the TS species (confined in the H-ZSM-5 zeolite) of the rate-determining step in a) the paring route and b) the side-chain methylation route. The isosurfaces of the reduced density gradient are colored according to the values of the quantity sign($\lambda 2$)ρ, and the RGB scale is indicated. VDW represents van der Waals interactions.

either effluent or extract products. All these results demonstrate that the side-chain methylation route is absent or at least negligible for the formation of propene though the steps from S1 to S5 are predicted to be kinetically feasible (with energy barriers being usually lower than 30 kcal mol^{-1}). As is known that the inter-conversion of light olefins can efficiently proceed, particularly under steady-state conditions.[10b, 30] Our experimental results have shown that the MBs formed in the induction period could provide the necessary propene through the paring route in the initial stage. The methanol conversion would subsequently proceed through a rapid C_{3+} olefin methylation/cracking as secondary reactions for the olefins formation. According to the theoretical calculation,[30] the repeated methylation/cracking of propene has an energy barrier of 14–19 kcal mol^{-1} for the formation of C_{3+} olefins, whereas it has 22–29 kcal mol^{-1} for producing ethene. Thus, these methylation/cracking processes involved in the alkene-based cycle are much more kinetically favorable than the paring route in the aromatic-based cycle for producing propene. Inevitably, the efficient methylation/cracking processes may compete with the paring route throughout the induction period and the subsequent steady-state period. This suggests that both the paring route and the methylation/cracking route play essential roles in the MTO chemistry over zeolite H-ZSM-5, with the former being mainly responsible for the initiation of the reaction, whereas the later significantly boosts the propene and C_{3+} olefin formation.

We have shown the critical role of the cyclic carbocations in the MTO reaction over the H-ZSM-5 zeolite. The frequently proposed MBs hydrocarbon pool can thus be reasonably connected by the cyclic carbocations to the olefin products. Generation of benzenium ions through *gem* methylation of aromatics is the starting point from which the MBs enter into the aromatics-based catalytic cycle. Proper channels or cages of the zeolites provide a spatial and chemical environment required for the formation and stabilization of special carbocations. Compared to C_5-cyclic cations, the C_6-cyclic cations are more space demanding, especially for the methyl-substituted carbocations. On zeolite SSZ-13 with a chabazite (CHA) topology that features a three-dimensional cage ($\approx 6.7 \times 10$ Å^2) structure with an eight-membered ring opening (3.8×3.8 Å^2), large carbocations such as the heptamethylbenzenium ion and the pentamethylcyclopentenyl cations were identified by NMR spectroscopy under steady-state conditions and linked to the formation of propene in the MTO reaction.[20] In this case, DFT calculations demonstrated that although both the paring and the side-chain methylation mechanism were energetically feasible reaction routes, the latter was more predominant owing to its much lower energy barrier.[20] The strong topological dependence of the cyclic carbenium ions has been theoretically addressed by the transition-state shape selectivity, which defines the specific carbenium ions.[31] The CHA topology of SSZ-13 with a larger spacious cage provides a favorable environment for the formation and stabilization of heptamethylbenzenium ions, whereas the geometric constraints imposed by a medium pore (sinusoidal channel: 5.5×5.1 Å^2, straight channel: 5.3×5.6 Å^2) of H-ZSM-5 only allows the pentamethylbenzenium ions

These are not the final page numbers! ↗↗

(i.e., cation **4**) to be present as the persistent species. On H-ZSM-5, the paring route involving the pentamethylbenzenium ions and the cyclopentenyl cations for the formation of propene is more favorable due to its lower energy barrier compared with the side-chain route, which is quite different to the MTO reaction mechanism on SSZ-13.

Finally, it should be pointed out that although our ^{13}C-labeling experiments support the paring route for producing ethene in the initial stage, its detailed pathway is still unclear from the present data. Thus, the observation and determination of the corresponding key carbocation intermediates is highly desirable for the elucidation of the detailed mechanism. Further work to clarify this issue is currently under way.

Conclusion

In summary, we have gained new insights into the hydrocarbon-pool chemistry of the MTO reaction over zeolite H-ZSM-5 from a combined experimental and theoretical investigation. We experimentally demonstrated the operation of an aromatics-based paring mechanism for the formation of propene, which was also theoretically supported by DFT calculations. In the initial stage of the MTO reaction, polymethylbenzenes were found to be the precursors of light olefins and mechanistically correlated to the formation of ethene and propene. Solid-state NMR spectroscopy confirmed the simultaneous formation of cyclopentenyl cations and the pentamethylbenzenium ion under both co-reaction ([^{13}C$_6$]benzene and methanol) conditions and typical MTO working conditions. Polymethylbenzenes and the carbocations work together to produce propene through a paring route, which involves a 6↔5 ring-contraction/expansion process. As demonstrated by DFT calculations, the propene formation step was the rate-determining step with a reasonable reaction barrier in a full catalytic cycle, providing a solid support for the paring route. In contrast, the side-chain methylation route, another frequently proposed mechanism for the formation of light olefins, was theoretically found to be less favorable for the formation of propene because of the high energy barrier required. These results presented herein shed new insight into the hydrocarbon-pool species and the detailed aromatics-based hydrocarbon-pool mechanism in the MTO reaction over zeolite H-ZSM-5, which might be helpful for the development of highly efficient MTO processes.

Experimental Section

Catalysis experiments

Methanol (weight hourly space velocity (WHSV) = 2 h^{-1}) was reacted over H-ZSM-5 (Si/Al = 30, 0.3 g) in a fixed bed reactor in a temperature range of 300–400 °C. In each case, the catalysts were compressed to wafers that were crushed and sieved to obtain 60–80 mesh particles, and then the particles were activated in place prior to the reaction by heating at 400 °C in flowing helium for 1 h. For the co-reaction of ^{13}C-labeled benzene (99 % ^{13}C, denoted as [^{13}C$_6$]benzene) with unlabeled methanol (^{13}C natural abundance, denoted as methanol), a pulse-quench reactor was used to quench

the reaction by reducing the reaction temperature with liquid nitrogen within a very short period (< 1 s).[32] Typically, when the reaction proceeded in a pulse-quench reactor for a pre-set period, the reaction was thermally quenched by pulsing liquid nitrogen onto the catalyst bed, which was achieved by using high-speed valves controlled by a GC computer. The molar ratio of methanol to [^{13}C$_6$]benzene was 2:1. In each case, an aliquot of the mixture (10 μL) was pulsed into the reactor (heated at 400 °C) containing H-ZSM-5 (0.3 g) and allowed to react for four, eight, and sixteen seconds, respectively before quenching by liquid nitrogen. The product distribution and the ^{13}C components in the effluent were determined by GC-MS analysis.

In ^{12}C/^{13}C methanol isotope transient experiments, ^{13}C natural abundance methanol was fed at 300 °C for 30 min before switching to [^{13}C]methanol (99 % ^{13}C) and was allowed to react for a variable period up to 4 min. The evolution of the ^{13}C components in the effluent was determined by GC-MS analysis after the [^{13}C]methanol switch at 1.0, 2.0 and 4.0 min. The corresponding isotopic data for the trapped species in the zeolite channels during the reaction were obtained.

Gas chromatography

The effluent was analyzed quantitatively by online GC (Shimadzu GC-2010 plus) equipped with a flame-ionization detector and a fused silica capillary column Petrocol DH100 (100 m, 0.25 mm i.d., 0.5 μm film thickness). The temperature programming started at 50 °C (maintained for 15 min), followed by a rate of 15 °C min^{-1} to a finial temperature of 200 °C. The isotopic compositions of the trapped species were analyzed by GC-MS (Shimadzu GCMS-QP2010) equipped with the same capillary column as GC analysis. The following temperature programming was applied: maintained at an initial temperature of 50 °C for 1 min, followed by a rate of 10 °C min^{-1} to a finial temperature of 250 °C (maintained for 10 min).

NMR experiments

After the reaction was quenched by liquid nitrogen, the reactor containing the catalyst sample was sealed. The sealed reactor was transferred to a glovebox filled with pure N$_2$ and the catalyst sample was packed into to an NMR rotor for NMR measurements. All solid-state NMR spectroscopy experiments were carried out at 11.7 T on a Bruker-Avance III-500 spectrometer, equipped with a 4 mm probe, with resonance frequencies of 500.57 and 125.87 MHz for ^{1}H and ^{13}C, respectively. Single-pulse ^{13}C MAS experiments with ^{1}H decoupling were performed by using a π/2 pulse width of 3.9 μs and a repetition time of 5 s. The magic-angle spinning rate was set to approximately 10.6–12.5 kHz. For the ^{1}H → ^{13}C CP/MAS NMR experiments, Hartmann–Hahn conditions were achieved by using hexamethylbenzene (HMB), with a contact time of 8 ms and a repetition time of 2 s. The ^{13}C chemical shifts were referenced to HMB (a second reference to TMS).

Theoretical details

A 72 T cluster model, which uses the extracted crystallographic data, was applied to represent the H-ZSM-5 zeolite, which contains the intersection of 10-membered ring straight and zigzag pore channels (Figure S9 in the Supporting Information). On the basis of the accessibility of adsorbed molecules toward the H-ZSM-5 zeolite, the Al$_{12}$-O$_{24}$H-Si$_{12}$ site in the intersection channel was chosen as the active center.[33] The terminal Si atoms were saturated with hydrogen atoms, and the hydrogen atoms were positioned on the

↖↖ These are not the final page numbers!

vector from the Si atom to the O atom that the hydrogen atom was replacing. All terminal Si–H bond lengths were set to 1.47 Å. The geometries of the carbocations **1–4** were optimized over the 72 T cluster model by the combined theoretical ONIOM (our-own-N-layered integrated molecular orbital and molecular mechanics) method. In the calculations, the carbocations and the high-layer atoms of the zeolite framework were allowed to fully relax with the latest ωB97XD functional with the 6-311G(d,p) basis set, whereas the rest atoms were fixed at their crystallographic positions with the AM1 method.[34] Based on the optimized structures, the ^{13}C NMR chemical shifts were then calculated at the ONIOM(MP2/6-311G(d,p):$\omega\omega$B97XD/6-311G(d,p)) level by the GIAO method.[35] The calculated ^{13}C NMR chemical shifts were all referenced to that of benzene ($\delta = 128.5$ ppm).

The ONIOM method was also applied to predict the geometries of the reactants, the transition states (TSs), and the products in the MTO reaction, which has been successfully used to explore the catalytic reactions over acidic zeolites.[24,31,36] The ONIOM (ωB97XD/6-31G(d,p):mndo) level of theory was utilized for the geometry optimizations,[37] where the (SiO)$_3$-Si-OH-Al-(SiO)$_3$ acid site and the adsorbed organic molecule were considered as the high-level layer, whereas the rest was considered as the low level. For all geometry optimizations, the atoms in the high level were allowed to fully relax, whereas the rest atoms were fixed at their crystallographic positions. The single-point energy calculations were further refined at the ωB97XD/6-31G(d,p) level. Frequency calculations were used to verify the optimized TS structures. All geometry optimizations and frequency calculations were performed by using the Gaussian 09 package.[38]

Acknowledgements

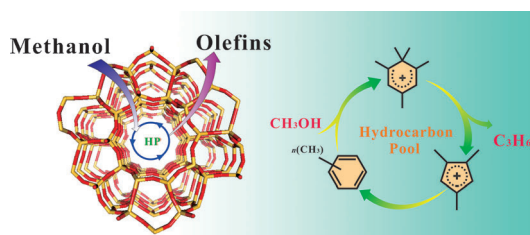**Keywords:** carbocations · olefins · reaction mechanisms · solid-state NMR spectroscopy · zeolites

[1] C. D. Chang, A. J. Silvestri, *J. Catal.* **1977**, *47*, 249–259.

[2] H. Koempel, W. Liebner, *Stud. Surf. Sci. Catal.* **2007**, *167*, 261–267.

[3] B. V. Vora, T. L. Marker, P. T. Barger, H. R. Nilsen, S. Kvisle, T. Fuglerud, *Stud. Surf. Sci. Catal.* **1997**, *107*, 87–98.

[4] a) M. Stöcker, *Microporous Mesoporous Mater.* **1999**, *29*, 3–48; b) J. F. Haw, W. G. Song, D. M. Marcus, J. B. Nicholas, *Acc. Chem. Res.* **2003**, *36*, 317–326; c) U. Olsbye, S. Svelle, M. Bjørgen, P. Beato, T. V. W. Janssens, F. Joensen, S. Bordiga, K. P. Lillerud, *Angew. Chem.* **2012**, *124*, 5910–5933; *Angew. Chem. Int. Ed.* **2012**, *51*, 5810–5831; d) K. Hemelsoet, J. Van der Mynsbrugge, K. De Wispelaere, M. Waroquier, V. Van Speybroeck, *ChemPhysChem* **2013**, *14*, 1526–1545; e) S. Ilias, A. Bhan, *ACS Catal.* **2013**, *3*, 18–31.

[5] a) W. Wang, Y. J. Jiang, M. Hunger, *Catal. Today* **2006**, *113*, 102–114; b) Y. J. Jiang, W. Wang, V. R. Reddy Marthala, J. Huang, B. Sulikowski, M. Hunger, *J. Catal.* **2006**, *238*, 21–27; c) W. Wang, A. Buchholz, M. Seiler, M. Hunger, *J. Am. Chem. Soc.* **2003**, *125*, 15260–15267.

[6] D. Lesthaeghe, V. Van Speybroeck, G. B. Marin, M. Waroquier, *Angew. Chem.* **2006**, *118*, 1746–1751; *Angew. Chem. Int. Ed.* **2006**, *45*, 1714–1719.

[7] D. M. Marcus, K. A. McLachlan, M. A. Wildman, J. O. Ehresmann, P. W. Kletnieks, J. F. Haw, *Angew. Chem.* **2006**, *118*, 3205–3208; *Angew. Chem. Int. Ed.* **2006**, *45*, 3133–3136.

[8] a) W. G. Song, D. M. Marcus, H. Fu, J. O. Ehresmann, J. F. Haw, *J. Am. Chem. Soc.* **2002**, *124*, 3844–3845; b) R. M. Dessau, R. B. LaPierre, *J. Catal.* **1982**, *78*, 136–141; c) R. M. Dessau, *J. Catal.* **1986**, *99*, 111–116; d) T. Mole, G. Bett, D. Seddon, *J. Catal.* **1983**, *84*, 435–445; e) T. Mole, J. A. Whiteside, D. Seddon, *J. Catal.* **1983**, *82*, 261–266; f) B. E. Langner, *Appl. Catal.* **1982**, *2*, 289–302.

[9] a) I. Dahl, S. Kolboe, *Catal. Lett.* **1993**, *20*, 329–336; b) I. M. Dahl, S. Kolboe, *J. Catal.* **1994**, *149*, 458–464; c) I. M. Dahl, S. Kolboe, *J. Catal.* **1996**, *161*, 304–309.

[10] a) S. Svelle, F. Joensen, J. Nerlov, U. Olsbye, K. P. Lillerud, S. Kolboe, M. Bjørgen, *J. Am. Chem. Soc.* **2006**, *128*, 14770–14771; b) M. Bjorgen, S. Svelle, F. Joensen, J. Nerlov, S. Kolboe, F. Bonino, L. Palumbo, S. Bordiga, U. Olsbye, *J. Catal.* **2007**, *249*, 195–207.

[11] S. Teketel, U. Olsbye, K. P. Lillerud, P. Beato, S. Svelle, *Microporous Mesoporous Mater.* **2010**, *136*, 33–41.

[12] M. Westgård Erichsen, S. Svelle, U. Olsbye, *J. Catal.* **2013**, *298*, 94–101.

[13] a) Ø. Mikkelsen, P. O. Rønning, S. Kolboe, *Microporous Mesoporous Mater.* **2000**, *40*, 95–113; b) B. Arstad, S. Kolboe, *Catal. Lett.* **2001**, *71*, 209–212; c) B. Arstad, S. Kolboe, *J. Am. Chem. Soc.* **2001**, *123*, 8137–8138; d) J. F. Haw, J. B. Nicholas, W. G. Song, F. Deng, Z. Wang, T. Xu, C. S. Heneghan, *J. Am. Chem. Soc.* **2000**, *122*, 4763–4775; e) W. G. Song, J. Nicholas, A. Sassi, J. F. Haw, *Catal. Lett.* **2002**, *81*, 49–53; f) M. Bjørgen, U. Olsbye, S. Kolboe, *J. Catal.* **2003**, *215*, 30–44; g) M. Bjørgen, U. Olsbye, D. Petersen, S. Kolboe, *J. Catal.* **2004**, *221*, 1–10; h) M. Bjørgen, U. Olsbye, S. Svelle, S. Kolboe, *Catal. Lett.* **2004**, *93*, 37–40; i) M. Bjørgen, F. Bonino, S. Kolboe, K. P. Lillerud, A. Zecchina, S. Bordiga, *J. Am. Chem. Soc.* **2003**, *125*, 15863–15868.

[14] a) P. W. Goguen, T. Xu, D. H. Barich, T. W. Skloss, W. G. Song, Z. K. Wang, J. B. Nicholas, J. F. Haw, *J. Am. Chem. Soc.* **1998**, *120*, 2650–2651; b) T. Xu, D. H. Barich, P. W. Goguen, W. G. Song, Z. K. Wang, J. B. Nicholas, J. F. Haw, *J. Am. Chem. Soc.* **1998**, *120*, 4025–4026.

[15] a) W. G. Song, H. Fu, J. F. Haw, *J. Am. Chem. Soc.* **2001**, *123*, 4749–4754; b) W. G. Song, J. F. Haw, J. B. Nicholas, C. S. Heneghan, *J. Am. Chem. Soc.* **2000**, *122*, 10726–10727; c) W. G. Song, H. Fu, J. F. Haw, *J. Phys. Chem. B* **2001**, *105*, 12839–12843; d) J. F. Haw, D. Marcus, *Top. Catal.* **2005**, *34*, 41–48; e) B. P. C. Hereijgers, F. Bleken, M. H. Nilsen, S. Svelle, K. P. Lillerud, M. Bjørgen, B. M. Weckhuysen, U. Olsbye, *J. Catal.* **2009**, *264*, 77–87.

[16] U. Olsbye, M. Bjørgen, S. Svelle, K. P. Lillerud, S. Kolboe, *Catal. Today* **2005**, *106*, 108–111.

[17] a) M. Seiler, W. Wang, A. Buchholz, M. Hunger, *Catal. Lett.* **2003**, *88*, 187–191; b) A. Sassi, M. A. Wildman, J. F. Haw, *J. Phys. Chem. B* **2002**, *106*, 8768–8773; c) A. Sassi, M. A. Wildman, H. J. Ahn, P. Prasad, J. B. Nicholas, J. F. Haw, *J. Phys. Chem. B* **2002**, *106*, 2294–2303.

[18] R. F. Sullivan, C. J. Egan, G. E. Langlois, R. P. Sieg, *J. Am. Chem. Soc.* **1961**, *83*, 1156–1160.

[19] a) J. Xu, A. M. Zheng, X. M. Wang, G. D. Qi, J. H. Su, J. Du, Z. H. Gan, J. F. Wu, W. Wang, F. Deng, *Chem. Sci.* **2012**, *3*, 2932–2940; b) X. M. Wang, G. D. Qi, J. Xu, B. J. Li, C. Wang, F. Deng, *Angew. Chem.* **2012**, *124*, 3916–3919; *Angew. Chem. Int. Ed.* **2012**, *51*, 3850–3853; c) I. I. Ivanova, Y. G. Kolyagin, *Chem. Soc. Rev.* **2010**, *39*, 5018–5050; d) M. Hunger, J. Weitkamp, *Angew. Chem.* **2001**, *113*, 3040–3059; *Angew. Chem. Int. Ed.* **2001**, *40*, 2954–2971.

[20] S. T. Xu, A. M. Zheng, Y. X. Wei, J. R. Chen, J. Z. Li, Y. Y. Chu, M. Z. Zhang, Q. Y. Wang, Y. Zhou, J. B. Wang, F. Deng, Z. M. Liu, *Angew. Chem.* **2013**, *125*, 11778–11782; *Angew. Chem. Int. Ed.* **2013**, *52*, 11564–11568.

[21] S. Ilias, A. Bhan, *J. Catal.* **2014**, *311*, 6–16.

[22] X. Y. Sun, S. Mueller, H. Shi, G. L. Haller, M. Sanchez-Sanchez, A. C. van Veen, J. A. Lercher, *J. Catal.* **2014**, *314*, 21–31.

[23] D. M. McCann, D. Lesthaeghe, P. W. Kletnieks, D. R. Guenther, M. J. Hayman, V. Van Speybroeck, M. Waroquier, J. F. Haw, *Angew. Chem.* **2008**, *120*, 5257–5260; *Angew. Chem. Int. Ed.* **2008**, *47*, 5179–5182.

[24] D. Lesthaeghe, A. Horré, M. Waroquier, G. B. Marin, V. Van Speybroeck, *Chem. Eur. J.* **2009**, *15*, 10803–10808.

[25] S. Svelle, P. O. Rønning, S. Kolboe, *J. Catal.* **2004**, *224*, 115–123.

[26] W. G. Song, J. B. Nicholas, J. F. Haw, *J. Phys. Chem. B* **2001**, *105*, 4317–4323.

[27] a) A. G. Stepanov, V. N. Sidelnikov, K. I. Zamaraev, *Chem. Eur. J.* **1996**, *2*, 157–167; b) J. F. Haw, B. R. Richardson, I. S. Oshiro, N. D. Lazo, J. A. Speed, *J. Am. Chem. Soc.* **1989**, *111*, 2052–2058.

[28] a) B. Arstad, J. B. Nicholas, J. F. Haw, *J. Am. Chem. Soc.* **2004**, *126*, 2991–3001; b) C. M. Wang, Y. D. Wang, Z. K. Xie, Z. P. Liu, *J. Phys. Chem. C*

2009, *113*, 4584 – 4591; c) K. De Wispelaere, K. Hemelsoet, M. Waroquier, V. Van Speybroeck, *J. Catal.* **2013**, *305*, 76 – 80.

[29] a) E. R. Johnson, S. Keinan, P. Mori-Sánchez, J. Contreras-García, A. J. Cohen, W. Yang, *J. Am. Chem. Soc.* **2010**, *132*, 6498 – 6506; b) W. M. Sun, R. Di Felice, *J. Phys. Chem. C* **2012**, *116*, 24954 – 24961.

[30] D. Lesthaeghe, J. van der Mynsbrugge, M. Vandichel, M. Waroquier, V. Van Speybroeck, *ChemCatChem* **2011**, *3*, 208 – 212.

[31] D. Lesthaeghe, B. De Sterck, V. Van Speybroeck, G. B. Marin, M. Waroquier, *Angew. Chem.* **2007**, *119*, 1333 – 1336; *Angew. Chem. Int. Ed.* **2007**, *46*, 1311 – 1314.

[32] J. F. Haw, P. W. Goguen, T. Xu, T. W. Skloss, W. G. Song, Z. K. Wang, *Angew. Chem.* **1998**, *110*, 993 – 995; *Angew. Chem. Int. Ed.* **1998**, *37*, 948 – 949.

[33] H. Van Koningsveld, H. Van Bekkum, J. C. Jansen, *Acta Crystallogr. Sect. B* **1987**, *43*, 127 – 132.

[34] M. J. S. Dewar, E. G. Zoebisch, E. F. Healy, J. J. P. Stewart, *J. Am. Chem. Soc.* **1985**, *107*, 3902 – 3909.

[35] K. Wolinski, J. F. Hinton, P. Pulay, *J. Am. Chem. Soc.* **1990**, *112*, 8251 – 8260.

[36] a) C. Tuma, J. Sauer, *Phys. Chem. Chem. Phys.* **2006**, *8*, 3955 – 3965; b) M. Boronat, C. Martínez-Sánchez, D. Law, A. Corma, *J. Am. Chem. Soc.* **2008**, *130*, 16316 – 16323.

[37] J. D. Chai, M. Head-Gordon, *Phys. Chem. Chem. Phys.* **2008**, *10*, 6615 – 6620.

[38] Gaussian 09, Revision B.01, M. J. Frisch, G. W. Trucks, H. B. Schlegel, G. E. Scuseria, M. A. Robb, J. R. Cheeseman, G. Scalmani, V. Barone, B. Mennucci, G. A. Petersson, H. Nakatsuji, M. Caricato, X. Li, H. P. Hratchian, A. F. Izmaylov, J. Bloino, G. Zheng, J. L. Sonnenberg, M. Hada, M. Ehara, K. Toyota, R. Fukuda, J. Hasegawa, M. Ishida, T. Nakajima, Y. Honda, O. Kitao, H. Nakai, T. Vreven, J. A. Montgomery, Jr., J. E. Peralta, F. Ogliaro, M. Bearpark, J. J. Heyd, E. Brothers, K. N. Kudin, V. N. Staroverov, R. Kobayashi, J. Normand, K. Raghavachari, A. Rendell, J. C. Burant, S. S. Iyengar, J. Tomasi, M. Cossi, N. Rega, J. M. Millam, M. Klene, J. E. Knox, J. B. Cross, V. Bakken, C. Adamo, J. Jaramillo, R. Gomperts, R. E. Stratmann, O. Yazyev, A. J. Austin, R. Cammi, C. Pomelli, J. W. Ochterski, R. L. Martin, K. Morokuma, V. G. Zakrzewski, G. A. Voth, P. Salvador, J. J. Dannenberg, S. Dapprich, A. D. Daniels, O. Farkas, J. B. Foresman, J. V. Ortiz, J. Cioslowski, D. J. Fox, Gaussian Inc., Wallingford CT, **2009**.

↖↖ These are not the final page numbers!

■ Hydrocarbon-Pool Chemistry

C. Wang, Y. Chu, A. Zheng, J. Xu,*
Q. Wang, P. Gao, G. Qi, Y. Gong, F. Deng*

■■ – ■■

New Insight into the Hydrocarbon-Pool Chemistry of the Methanol-to-Olefins Conversion over Zeolite H-ZSM-5 from GC-MS, Solid-State NMR Spectroscopy, and DFT Calculations

Pool party! The aromatic-based hydrocarbon-pool (HP) chemistry in the methanol-to-olefins (MTO) reaction over zeolite H-ZSM-5 was studied by a combined experimental and theoretical calculation approach (see figure). Polymethylbenzenes and the carbocations (trimethyl-cyclopentenyl and pentamethylbenzium ions) serve as active hydrocarbon-pool species and work together through a paring route to produce propene in an aromatic-based catalytic cycle.

Hydrocarbon-Pool Chemistry

Hydrocarbon-pool chemistry plays a critical role in methanol-to-olefins reaction, but in depth understanding of the reaction pathway still remains a big challenge. Over archetype H-ZSM-5 zeolite, the observation and identification of carbocations is reported under working conditions. A paring route for producing propene in an aromatic-based catalytic cycle is described by connecting the polymethylbenzenes and the carbocations. For more detail, see the full paper by J. Xu, F. Deng et al. on page ■■ ff..

These are not the final page numbers! ↗↗